Development 128, 4079-4092 (2001)
Printed in Great Britain © The Company of Biologists Limited 2001
DEV8759

UNC-119 suppresses axon branching in *C. elegans*

Karla M. Knobel‡, Warren S. Davis, Erik M. Jorgensen* and Michael J. Bastiani

Department of Biology, University of Utah, 257 South 1400 East, Salt Lake City, UT 84112-0840, USA
‡Present address: School of Pharmacy, University of Wisconsin, 777 Highland Avenue, Madison, WI 53705-2222, USA
*Author for correspondence (e-mail: jorgensen@biology.utah.edu)

Accepted 24 July 2001

SUMMARY

The architecture of the differentiated nervous system is stable but the molecular mechanisms that are required for stabilization are unknown. We characterized the gene *unc-119* in the nematode *Caenorhabditis elegans* and demonstrate that it is required to stabilize the differentiated structure of the nervous system. In *unc-119* mutants, motor neuron commissures are excessively branched in adults. However, live imaging demonstrated that growth cone behavior during extension was fairly normal with the exception that the overall rate of migration was reduced. Later, after development was complete, secondary growth cones sprouted from existing motor neuron axons and cell bodies. These new growth cones extended supernumerary branches to the dorsal nerve cord at the same time the previously formed axons retracted. These defects could be suppressed by expressing the UNC-119 protein after embryonic development; thus demonstrating that UNC-119 is required for the maintenance of the nervous system architecture. Finally, UNC-119 is located in neuron cell bodies and axons and acts cell-autonomously to inhibit axon branching.

Key words: Growth cone, Axon branching, Sprouting, Neuron stabilization, *unc-119*, *Caenorhabditis elegans*

INTRODUCTION

Typically, mature neurons are polarized cells composed of a dendritic arbor and a single axon (reviewed by Craig and Banker, 1994; Higgins et al., 1997). This polarity becomes apparent early during development when the neuron extends a growth cone to form a single unbranched axon (reviewed by Goodman, 1996; Goodman and Tessier-Lavigne, 1997; Mueller, 1999). In some neuronal populations collateral branches project from axons after the growth cone has reached its primary target (O'Leary and Terashima, 1988; O'Leary, 1992; Bastmeyer and O'Leary, 1996). The growth cones of other neurons bifurcate during extension (Bray, 1973; Bunge, 1973). Once the growth cone reaches its target, functional synapses are established at the tip of the axon (reviewed by Sanes and Scheller, 1997; Sanes and Lichtman, 1999) and the differentiated neuron stops growing. The stability of the differentiated nervous system can be perturbed by nerve injury or disease, resulting in abnormal axon branching (Lankford et al., 1998; Stoll and Muller, 1999). Similarly, the induction of epileptic seizures in experimental animals results in over-production of axon collateral sprouts (reviewed by McNamara, 1999). While a variety of molecules stimulate branching during regeneration (Ernfors et al., 1991; Bendotti et al., 1993; Aguayo et al., 1996; Caroni, 1998), the molecular mechanisms inhibiting branching are largely unknown.

We have discovered that a new molecule, UNC-119, suppresses abnormal axon branching. *unc-119* was originally identified as a mutation affecting nematode locomotion (Maduro and Pilgrim, 1995). The *unc-119* transcript is expressed primarily in neurons early in development and throughout adulthood (Maduro and Pilgrim, 1995). UNC-119 does not contain any well-defined structural motifs, although several proteins that are similar to UNC-119 have been identified in *C. elegans*, *Drosophila melanogaster* and vertebrates (Maduro et al., 2000). Two related vertebrate proteins, HRG4 (human UNC119) and RRG4 (rat UNC119), were recently identified based on their high level of gene expression in the retina (Higashide, 1996; Swanson et al., 1998). Specifically, these proteins are localized to the presynaptic zone of the retinal ribbon synapses (Higashide, 1998). The human homolog, HRG4 was recently mapped to 17q11.2 (Swanson et al., 1998; Higashide and Inana, 1999). The function of the UNC-119 protein family members has not yet been determined.

Here we demonstrate that GABA motor neuron axons are severely branched in adult *unc-119* mutants and synapses are inappropriately localized. Axon branching in *unc-119* mutants could result from defects that occur before, during or after outgrowth. Time-lapse analyses of *unc-119* growth cones demonstrated that, despite timing defects, the behaviors exhibited by GABA motor neuron axons during migration are normal. Instead, motor axon branching occurred *after* axon outgrowth and was the result of supernumerary growth cone activity. Transient expression of UNC-119 protein after outgrowth rescued the *unc-119* phenotype. Together these results suggest that the UNC-119 protein maintains the differentiated morphology of the neuron by suppressing supernumerary axon branching and restricting the distribution of synapses.

MATERIALS AND METHODS

Strains and manipulations

Strain maintenance was performed as described previously (Brenner, 1974). *C. elegans* strain EG1285 *lin-15(n765ts) oxIs12* [*Punc-47*::GFP NTX, EK L15 (*lin-15(+)*] X (McIntire et al., 1997) was crossed with *unc-119(ed3)* to generate EG1322: *unc-119(ed3)*III*; lin-15(n765ts) oxIs12* X. We generated an *unc-119(e2498)*III*; lin-15(n765ts) oxIs12* X (EG1705) strain and confirmed that the axon outgrowth phenotype of *unc-119(e2498)* was similar to that of *unc-119(ed3)*. The experiments described in this paper use EG1285 as wild-type and EG1322 as *unc-119(ed3)* unless otherwise indicated.

Scoring D-type motor neuron axon defects

Wild-type (EG1285) and *unc-119(ed3)* (EG1322*)* worms were collected within 30 minutes of hatching and raised at 20°C to particular stages during larval development. At 1 hour or 48 hours after hatching, larvae were mounted on agarose pads containing 10 mM NaN_3 (Knobel et al., 1999) and the morphology of the D-type GABA motor neurons was scored using fluorescence microscopy. At both timepoints we could distinguish between the DD and VD neurons because of the location of the cell bodies and axons along the ventral nerve cord. Moreover, DD axons expressing *Punc-47::GFP* (*oxIs12)* were brighter under fluorescence illumination than VD axons. The morphologies of DD axons were evaluated after outgrowth of the primary growth cone was complete. Axon morphologies were categorized as: (1) normal (these reached and bifurcated at the dorsal midline and then extended along the anteroposterior axis); (2) extension defective (reached the dorsal midline but failed to bifurcate and extend along the anteroposterior axis); (3) branched (contained multiple branches that extended to the dorsal midline); or (4) terminated (axons and branches failed to reach the dorsal nerve cord). Finally, we noted if there were supernumerary growth cones extending directly from DD cell bodies.

UNC-119 immunocytochemistry

To determine where the UNC-119 protein was located, we generated antibodies against UNC-119. The DNA encoding the N-terminal 48 amino acids of UNC-119 was subcloned into the pGEX-3X cloning vector (Pharmacia) to produce GST:Nu119 (pKK20). Bacteria were transformed with pKK20 and induced to express the fusion protein with 1 mM IPTG. Bacteria were grown at 37°C for two hours, harvested, washed and sonicated to separate soluble proteins from the membrane fraction. The GST:Nu119 fusion protein was isolated from the soluble fraction. GST:Nu119 was purified on a Glutathione Sepharose™ column (Pharmacia), lyophilized, and injected into rats to produce antisera against the fusion protein (Pokono Rabbit Farms and Laboratory). The GST:Nu119 antibody was purified from antisera by binding and removal from a CnBr-activated Sepharose™ column (Pharmacia) containing immobilized GST:Nu119. For immunocytochemical labeling wild-type adults were isolated, immobilized on siliconized coverslips and dissected (Richmond and Jorgensen, 1999). Worms were fixed for 1 hour at room temperature in fresh 2% paraformaldehyde, washed and placed briefly in pre-block (10% fetal calf serum in PGT: 1× PBS, 0.25% Triton X-100, 0.1% gelatin). Fixed worms were washed, incubated with antibody overnight at 4°C, washed again, and incubated in secondary antibody (Alexa Fluor™ 568 goat anti-rat IgG; Molecular Probes) for 1 hour at room temperature. After washing, worms were mounted and examined using a BioRad Radiance Laser 2000 laser scanning confocal microscope.

unc-119 rescue experiments

A *Punc-47*::UNC-119genomic:GFP construct was prepared by PCR amplifying plasmid DP#MM016 containing genomic DNA encoding UNC-119 (Maduro and Pilgrim, 1995) using primers containing novel *Bam*HI (5′ N-U119: 5′-CGGGGATCCATGAAGGCAGAGCAACAA-3′) and *Kpn*I (3′, C-U119: 5′-GACTACTCGTATGATGCAGAG-GTACCCC-3′) sites. The plasmid pJL35, containing *Punc-47*::synaptobrevin:GFP, was digested with *Bam*HI and *Kpn*I and gel purified to remove the synaptobrevin fragment, which was replaced by the digested PCR product encoding genomic UNC-119. The resulting ligation product, *Punc-47*::UNC-119genomic:GFP (pKK11) contained the GFP reporter fused in frame to the C terminus of the full-length UNC-119 protein. Similarly, the *Punc-47*::UNC-119cDNA:GFP (pKK12) reporter was prepared by PCR amplifying a fragment from the plasmid ‘*unc-119* cDNA5′ using these same primers. Ligations were performed as with pKK11. *Punc-47*::UNC-119cDNA:GFP (pKK12) contained the GFP reporter fused in frame to the C terminus of a cDNA minigene encoding the full-length UNC-119. All constructs were sequenced to check for errors introduced into our constructs by PCR. Transgenic strains expressing pKK11 or pKK12 (60 ng/μl) and EK L15 (*lin-15+* DNA; 60 ng/μl) plasmid DNA were generated by microinjection into *unc-119(ed3); lin-15(n765ts)* or *lin-15(n765ts)* mutants (Mello et al., 1991). F_1 progeny with a wild-type vulval phenotype were selected and scored for GFP expression using fluorescence microscopy. *unc-119(ed3); lin-15(n765ts) oxEx150* [pKK11; EK L15] and *lin-15(n765ts) oxEx267*[pKK11; EK L15] were generated in this manner. We generated *unc-119(ed3); lin-15(n765ts) oxEx151*[pKK12; EK L15] and then outcrossed this strain to produce *lin-15(n765ts) oxEx151*[pKK12; EK L15]. All strains were scored for rescue of GABA motor neuron outgrowth, generation time and locomotion. Interestingly, inclusion of *unc-119* introns in the GABA neuron expression construct (pKK11) rescued most of the locomotory phenotype of *unc-119(ed3); lin-15(n765ts) oxEx150* mutants. This rescue is likely to be the result of expression of GFP-tagged UNC-119 in several unidentified head neurons in these strains. Expression in these cells was probably caused by enhancers found in the introns of the genomic construct, since such expression did not occur in *unc-119(ed3); lin-15(n765ts) oxEx151*.

To determine the structure of other neurons in *unc-119(ed3)* mutants, we analyzed the CAN neuron in the lateral cord and the DB neurons in the ventral cord using *Pacr-5*::GAP-43:GFP (pJL1), and the A- and B-type motor neurons using *Paex-3*::SPECTRIN:GFP (pMH50). We crossed the extrachromosomal arrays *oxEx81*[pJL1 (30 ng/μl); EK L15 (60 ng/μl)] and *oxEx287*[pMH50 (30 ng/μl); EK L15 (60 ng/μl)] into *unc-119(ed3)* III; *lin-15(n765ts)* and characterized the outgrowth pattern of these neurons using confocal microscopy. To determine if other subsets of neurons were rescued by GFP-tagged UNC-119 expression in the GABA neurons we crossed transgenic animals expressing *oxEx151*[pKK12; EK L15] with worms expressing *oxEx81*[pJL1; EK L15] and isolated cross progeny. Thus, the *unc-119 (ed3); lin-15(n765ts)*; *oxEx81*[pJL1; EK L15]; *oxEx151* [pKK12; EK L15] (EG2440) and *lin-15(n765ts)*; *oxEx81*[pJL1; EK L15]; *oxEx151*[pKK12; EK L15] (EG2441) strains were generated. We characterized the axon morphology of the GABA motor neurons using *Punc-47*::UNC-119:GFP (*oxEx151*) and the CAN lateral cord neuron using *Pacr-5*::GAP-43:GFP (*oxEx81*) with confocal microscopy.

We failed to detect the circumferential extensions of DB motor neurons in *unc-119(ed3)* mutants expressing *Pacr-5*::GFP (Fig. 3B-D). We characterized the morphology of the cholinergic motor axons in *unc-119(ed3)* mutants expressing a pan-neuronal marker *Paex-3*::SPECTRIN:GFP. In both wild-type and mutant worms expressing this marker the DB motor axons extended to the dorsal nerve cord. In *unc-119(ed3)* mutants the DB axons exhibited minor branching defects in 75% of the worms scored (n=8 worms, data not shown). These data indicate that the defects in DB axon extension observed using the *Pacr-5*::GFP marker were caused by expression of the *Pacr-5*::GFP marker in the *unc-119(ed3)* strain and are *not* caused by mutations in the *unc-119* gene.

unc-119 time-lapse confocal microscopy

Wild-type and *unc-119(ed3)* larvae were collected within 30 minutes of hatching and incubated at 20°C. Staged larvae were then mounted on agarose pads made on a microscope slide. The slides were covered and sealed as described previously (Knobel et al., 1999). To image VD growth cones and DD axons we used either a BioRad MRC 600 or a BioRad Radiance Laser 2000 laser-scanning confocal microscope. Z-series were collected at various time intervals from 2 minutes to 20 minutes (Knobel et al., 1999). Appropriate sections were projected, and these Bio-Rad confocal '.pic' files were converted into TIF files and manipulated using Adobe PhotoShop™ and the public domain software package NIH Image. Quicktime movies were made from stacked files in NIH Image.

Rescue of *unc-119(ed3)* axon morphology using heat-shock promoters

Two constructs expressing UNC-119 in a regulated manner (*Phsp16-48*::UNC-119 and *Phsp16-2*::UNC-119) were generated by subcloning the *unc-119* cDNA into constructs containing the separate heat-shock promoters (pJL26: *Phsp16-48*, pPD49.78: *Phsp16-2*). The *hsp16-48* promoter is strongly expressed in the developing embryo (Stringham et al., 1992), and the *hsp16-2* promoter drives expression in neural and hypodermal cells (Mello and Fire, 1995). Transgenic *unc-119(ed3)* worms carrying either the *Phsp16-48* construct (*oxEx321*) or the *Phsp16-2* construct (*oxEx322*) and a marker were generated by co-injection. Injection mixes included a heat-shock construct at 2 ng/μl, herring sperm DNA at 40 ng/μl and marker DNA at 60 ng/μl. The marker, pPD97/98 is expressed in coelomocytes (Miyabayashi et al., 1999).

Heat-shock experiments were performed as follows. Animals in all groups were maintained at 20°C, heat shocked at 33°C for 1 hour, and returned to 20°C to develop. We maintained non-heat-shocked siblings as controls. Transgenic embryos were collected from gravid adults en masse and heat shocked (Lewis and Fleming, 1995). Newly hatched larvae were collected within 2 hours of heat shock (late embryonic heat-shock group) and 10 hours after embryonic heat shock (early embryonic heat-shock group). For the larval heat-shock experiments, embryos were collected and hatched in M9. Staged L1 larvae were heat shocked 24 hours later when all larvae had arrested development (corresponding to a stage equivalent to 3-5 hours after hatching). These animals were placed on plates with food and allowed to develop a few hours (L1 group). Non-heat-shocked sibling larvae were also allowed to develop for an additional 30-36 hours after hatching before being heat shocked as L3s (L3 group). For all groups (including non-heat-shocked controls) the morphologies of the DD axons were scored in worms expressing the co-injection marker at the L1, L2, L4, and adult stage of development. Data were combined from both heat-shock promoters and analyzed using the unpaired Student's *t*-test. Nearly complete rescue could be obtained by increasing the concentration of the heat-shock construct. However, we observed that at these concentrations leaky expression resulted in morphological rescue of non-heat-shocked controls. We did not include these data in our results.

Synapse analysis

Presynaptic varicosities in wild-type and *unc-119(ed3)* worms were characterized using the synapse markers *Punc-25*::synaptobrevin:GFP (*juIs1*) (Hallam and Jin, 1998; Nonet, 1999), *Pstr-3*::synaptobrevin:GFP (*kyIs105*; a gift from C. Bargmann and G. Crump), and *Pmec-7*::synaptobrevin:GFP (*jsIs37*) (Nonet, 1999). The following strains were evaluated using confocal microscopy: *unc-119(ed3)* III*; juIs1 lin-15(n765ts)* X (EG1978); *unc-119(ed3)* III*; kyIs105* V; *lin-15(n765ts)* X (EG1460) and *unc-119(ed3)* III*; jsIs37; lin-15(n765ts)* X (EG1885*)*. We characterized DD synapse localization in L1 larvae isolated within 1 hour of hatching and VD synapse localization in L3 larvae using fluorescence confocal microscopy. GABA motor neuron synapses were evaluated in the region of the anterior reflex of the gonad, and PLM synapses posterior of the vulva were evaluated. Data was analyzed for significance using unpaired Student's *t*-tests. We characterized the structure of $GABA_A$ receptor clusters in *oxIs22; lin-15(n765ts)*(EG1653) and *unc-119(ed3); oxIs22; lin-15(n765ts)* (EG1790) using an integrated *Punc-49*::UNC-49B:GFP marker (*oxIs22*) (Bamber et al., 1999).

Electron microscopy

Adult nematodes were prepared for transmission electron microscopy as described (Richmond et al., 1999). Specimens were immersed in ice cold fixative (0.7% glutaraldehyde/0.7% osmium tetroxide in 10 mM Hepes buffer) for 1 hour. Animals were then washed thoroughly in buffer and anterior and posterior extremities were excised in buffer. Postfixation was in 2% osmium tetroxide in 10 mM Hepes buffer for 3 hours. Specimens were then washed in water, stained en bloc in 1% uranyl acetate, dehydrated through an ethanol series, passed through propylene oxide and embedded in epoxy resin. Ribbons of ultrathin sections (~35 nm) were collected and examined on an Hitachi H-7100 TEM equipped with a Gatan slow-scan digital camera. Morphometric analysis was performed using the public domain software package NIH Image. For analysis, an active zone was defined as the set of serial sections containing a discernable presynaptic density, as well as two adjacent sections anterior and posterior to the sections containing the density. Docked vesicles were defined as those vesicles appearing within a single vesicle radius (~30 μm) of the presynaptic plasma membrane. Significance values were calculated using Student's *t*-tests or Wilcoxin rank-sum tests.

RESULTS

Motor neuron axons are branched in *unc-119* mutants

unc-119(ed3) mutants are extremely uncoordinated (Maduro and Pilgrim, 1995). We characterized the structure of the GABA nervous system in *unc-119(ed3)* and *unc-119(e2498)* mutants to determine if axon outgrowth defects contributed to the locomotory phenotype. We describe the results obtained with the *unc-119(ed3)* mutant although the morphological defects observed in both alleles were similar. We used the *unc-47* promoter (McIntire et al., 1997) to drive the expression of GFP (Chalfie et al., 1994) in all of the GABA neurons. In wild-type worms, the six embryonic DD and 13 larval VD motor neurons extend growth cones circumferentially from the ventral nerve cord to the dorsal nerve cord (Knobel et al., 1999). At the dorsal midline these axons bifurcate and extend anterior and posterior processes to form a contiguous dorsal nerve cord. In wild-type young adults scored at 38 hours after hatching, all DD and VD motor neuron axons had reached, bifurcated and extended along the dorsal midline (Fig. 1A,C; *n*=21 worms, 273 axons scored). In *unc-119(ed3)* animals scored at 38 hours after hatching, the GABA motor neuron cell bodies were located at normal positions and most D-type axons reached the dorsal nerve cord (Fig. 1B; 88% axons reach the dorsal nerve cord, *n*=9 worms, 144 axons scored). However, only a minority of the motor neuron axons were morphologically normal (Fig. 1C; 27%). Many of the axons in *unc-119(ed3)* mutants either failed to bifurcate and extend along the dorsal midline (Fig. 1C; 30% 'extension defective') or they were branched (Fig. 1C; 31%). Axons possessing supernumerary branches rarely extended processes along the dorsal nerve cord. As a consequence there were large gaps along the dorsal nerve cords. Finally, 15% of *unc-119(ed3)*

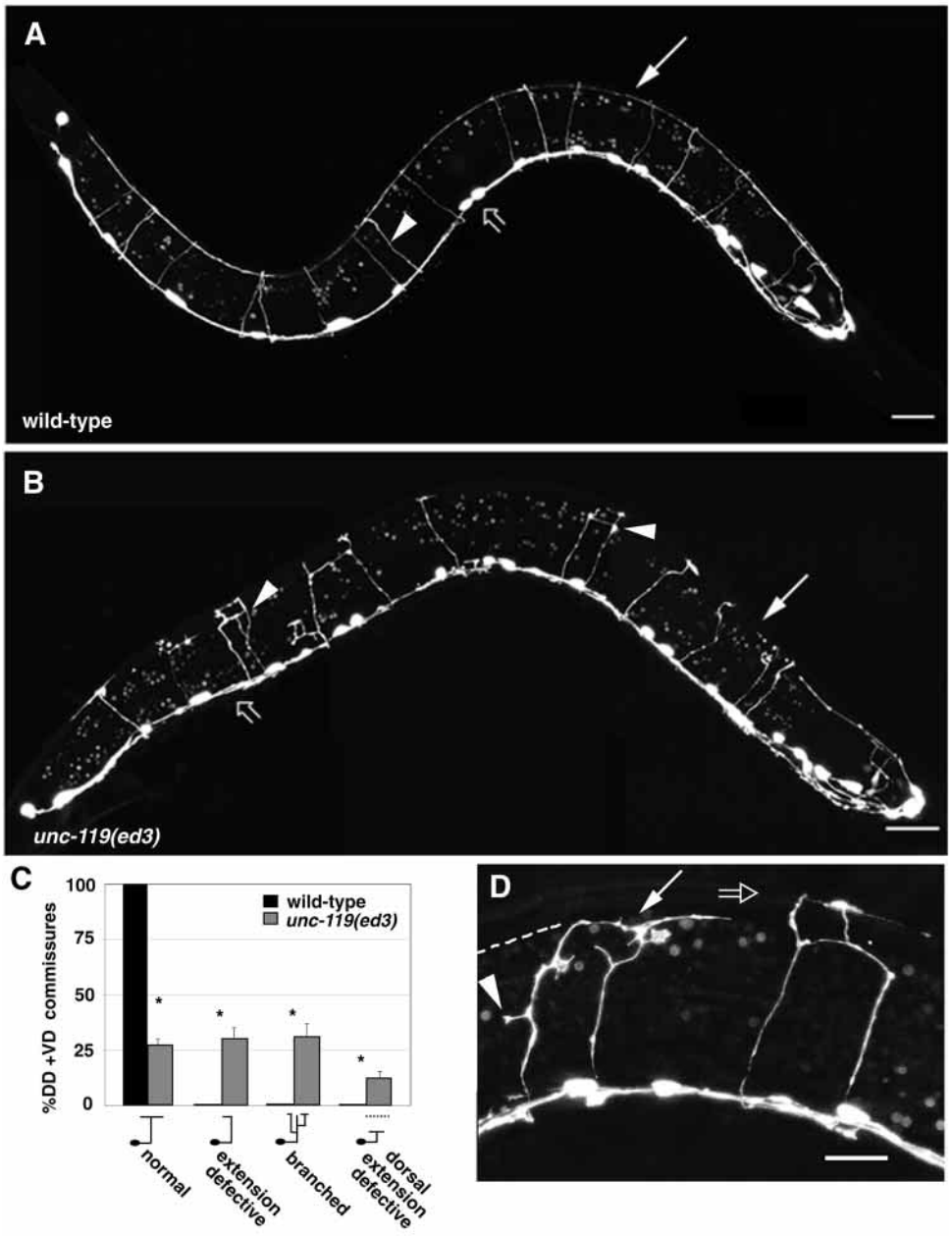

Fig. 1. *unc-119(ed3)* mutants have branched motorneuron axons. (A) Confocal micrograph of a wild-type young adult (38 hours after hatching) expressing GFP in GABA neurons. Anterior is to the right; posterior to the left. GFP was expressed in 19 D-type motorneuron cell bodies located along the tightly fasciculated ventral nerve cord (open arrow) and their commissures (arrowhead). The dorsal nerve cord was contiguous along the length of the animal (arrow). (B) Confocal micrograph of an *unc-119(ed3)* young adult expressing GFP in GABA neurons. There were branches in many of the axons that reached the dorsal cord (arrowheads), and large gaps in the dorsal nerve cord (solid arrow). The ventral nerve cord was defasciculated (open arrow). (C) GABA motor neuron structure was abnormal in *unc-119(ed3)* mutants scored at 38 hours after hatching. All wild-type axons were normal (left, n=21 worms, 273 axons). Although some *unc-119(ed3)* axons were normal (left, 27% ±2.8, n=9 worms, 144 axons), many reached the dorsal midline but failed to extend normally along the dorsal nerve cord (middle left, 30% ±3.9), many axons were branched (middle right, 31% ±6.0), and some axons failed to reach the dorsal nerve cord (right, 12.3% ±3.0). These differences from wild-type are significant (asterisk *, P<0.0001, t-test; error bars represent standard error of the mean). (D) Confocal micrograph of *unc-119(ed3)* axons branching at the dorsal body wall muscle. Brightfield illumination revealed the border between muscle and intestine (dotted line). Axons branched at the muscle (arrow) and at the lateral nerve cord (arrowhead). The dorsal nerve cord is marked by an open arrow. Scale bars (A,B) 25 μm, (C) 10 μm.

adults possessed extra motor neuron commissures extending from the ventral nerve cord. In summary, we observed that many motor neuron axons in *unc-119(ed3)* mutants were branched and that most axons failed to extend along the dorsal midline.

Interestingly, the abnormal axon branches observed in *unc-119(ed3)* mutants were located primarily at substrate boundaries (Knobel et al., 1999). Specifically, axon branches were initiated in regions where the growth cone encounters physical boundaries, such as the lateral nerve cord or the dorsal body wall muscle (Fig. 1D). The majority of axon branches were located at the dorsal body wall muscle (86%); the remaining branches were formed at the lateral or sublateral nerve cords. In many cases, branches extended from multiple locations along a single axon. Branched axons were never observed in wild-type animals.

UNC-119 protein is located in axons

Previous experiments using the *unc-119* promoter to drive the expression of reporter constructs demonstrated that the *unc-119* gene is expressed primarily in neurons (Maduro and Pilgrim, 1995). However, we were unable to detect any subcellular localization using our GFP-tagged UNC-119 constructs. To determine the subcellular location of UNC-119 we generated antibodies recognizing the N terminus of the protein. The nerve cords and axons of wild-type worms were labeled with purified antibodies (Fig. 2). Immunoreactivity was absent in *unc-119(ed3)* animals, and anti-UNC-119 antibodies exclusively labeled the GABA neurons expressing GFP-tagged UNC-119 protein in transgenic *unc-119(ed3)* (data not shown). Thus, the antibody is specific for UNC-119. UNC-119 immunoreactivity was not restricted to a specific subcellular location although the labeling was enriched in

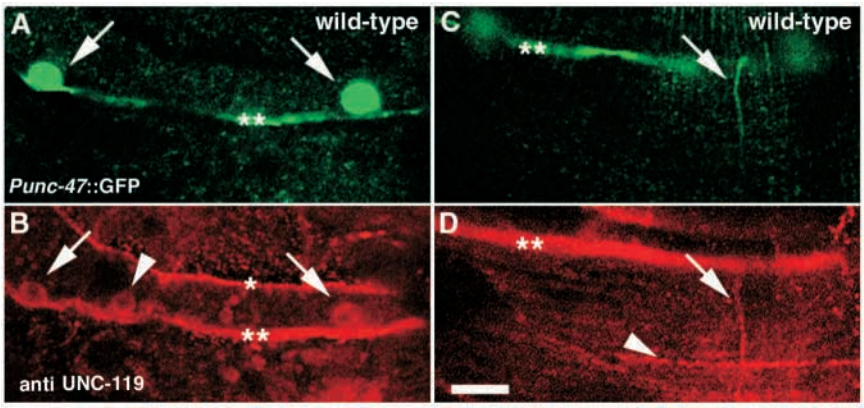

Fig. 2. UNC-119 is expressed in neurons. (A) GFP was expressed in the GABA motorneuron cell bodies (arrows) and axons (**) in a wild-type worm expressing a P*unc-47*::GFP construct. (B) In the same wild-type individual, anti-UNC-119 antibodies labeled multiple cell bodies (arrowhead and arrows) and axons in the left (*) and right (**) ventral nerve cords. (C) GFP was also expressed in the GABA motorneuron commissures of wild-type worm carrying a P*unc-47*::GFP construct (right ventral nerve cord: **, axon: arrow). (D) Anti-UNC-119 antibodies labeled the axons in the right ventral nerve cord (**), the commissures seen in (C, arrow), and the lateral nerve cord (arrowhead). Scale bar (A-D) 5 μm.

axonal processes and weakly expressed in the cytoplasm of neuronal cell bodies.

UNC-119 functions in neurons

The branching defects observed in *unc-119(ed3)* mutants could be caused by defects in axonal substrates, by changes in communication between neurons, or by cell intrinsic defects within neurons. We demonstrated that UNC-119 functions cell-autonomously by expressing a GFP-tagged UNC-119 protein in the GABA neurons of *unc-119(ed3)* mutants. Axonal morphology was restored *only* in the neurons expressing the fusion protein. Specifically, the promoter of the *unc-47* gene was used to express UNC-119 in the D-type GABA neurons (McIntire et al., 1997). The GFP-tagged UNC-119 protein was created by fusing the GFP coding region to the 3′ end of either the genomic region of the *unc-119* gene or a minigene constructed from the *unc-119* cDNA. When either of these constructs were expressed in *unc-119(ed3)* mutants the morphologies of the DD and VD GABA motor neurons were restored (Fig. 3A,E; *Punc-47*::UNC-119cDNA:GFP: 85%±7.3 normal axons, *n*=10 worms, 96 axons, data shown; *Punc-47*::UNC-119genomic:GFP: 83.8% normal axons ±4.8 rescued, *n*=8 worms, 79 axons, data not shown). Because expression of UNC-119 in the GABA neurons rescued

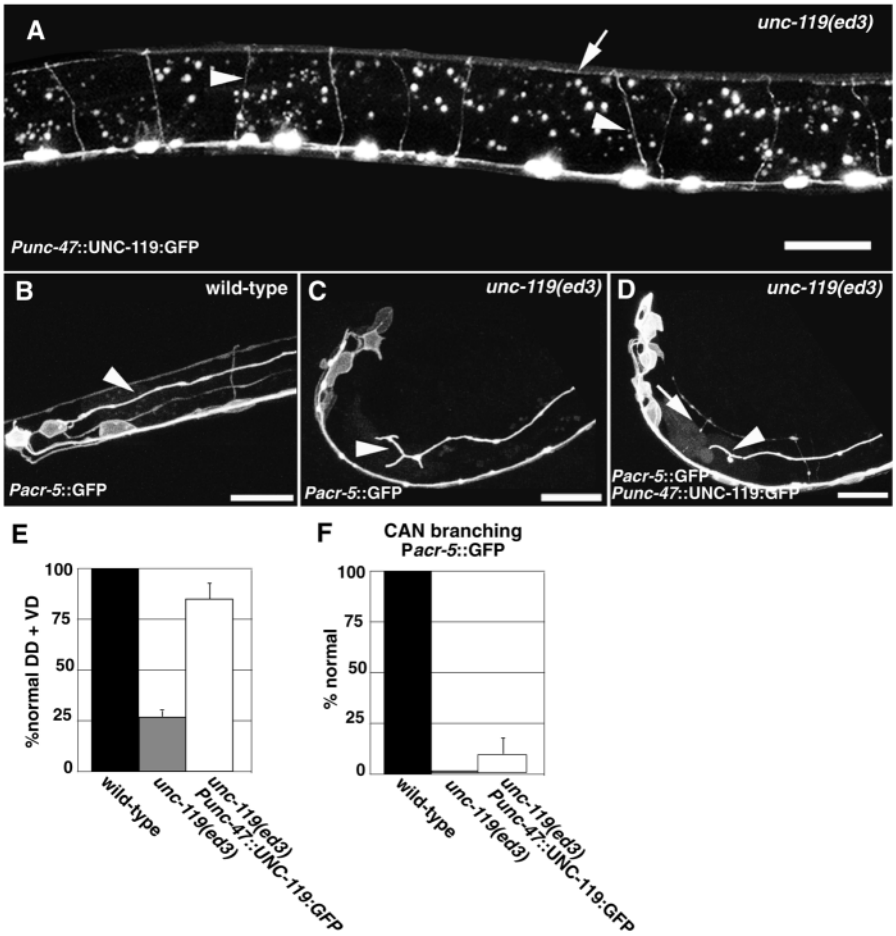

Fig. 3. UNC-119 functions cell-autonomously to suppress axon branching. (A) Expression of a GFP-tagged UNC-119 protein in the GABA motor neurons of an *unc-119(ed3)* mutant restored GABA motor axon structure (arrowheads). Note that there were no gaps in the dorsal nerve cord (arrow). (B) GFP expression in the CAN lateral cord neurons (arrowhead) of wild-type animals. The lateral cord axons were not branched. (C) The CAN axons of *unc-119(ed3)* mutants were branched (arrowhead). (D) Expression of a GFP-tagged UNC-119 protein in the GABA neurons of *unc-119(ed3)* mutants (left arrow) failed to rescue the branching of the CAN axons (arrowhead). (E) 100% of D-type motor neuron axons in wild-type worms were morphologically normal (black, *n*=16 worms, 96 axons). Only 27% ±2.8 of VD and DD axons were normal in *unc-119(ed3)* mutants (gray, *n*=9 worms, 144 axons). Expression of a GFP-tagged UNC-119 protein in the GABA neurons of *unc-119(ed3)* mutants restored the morphology of the DD and VD axons (white, 85% ±7.3, *n*=10 worms, 95 axons). (F) 100% of wild-type worms scored had unbranched lateral nerve cord CAN axons (black, *n*=12 worms). All of *unc-119(ed3)* mutants scored had branched CAN axons (gray, *n*=10 worms). Expression of a GFP-tagged UNC-119 protein in the GABA neurons of *unc-119(ed3)* mutants failed to rescue the branched morphology of the CAN axons (white, 8% *n*=13 worms). Scale bars (A-D) 10 μm.

outgrowth defects in these neurons we concluded that UNC-119 acts cell intrinsically. However, these data do not exclude the possibility that UNC-119 can rescue outgrowth defects nonautonomously. To determine whether UNC-119 could act nonautonomously we scored outgrowth defects of the lateral cord neurons and cholinergic motor neurons in transgenic *unc-119(ed3)* mutants expressing UNC-119 in the GABA neurons. The axons of the CAN neurons in the lateral cord were visualized using a *Pacr-5*::GFP construct. *acr-5* encodes an acetylcholine receptor subunit expressed in these cells (Winnier et al., 1999). We observed that lateral nerve cords were normal in wild-type worms and branched in 100% of *unc-119(ed3)* mutants expressing *Pacr-5*::GFP (Fig. 3B,C,F). Expression of UNC-119 in the GABA neurons failed to eliminate the branching defect of the lateral cord axons in transgenic *unc-119(ed3)* mutants expressing *Pacr-5*::GFP (Fig. 3D). Only 8% of *unc-119(ed3)* worms expressing both *Punc-47*::UNC-119:GFP and *Pacr-5*::GFP had morphologically normal lateral nerve cords (Fig. 3F) indicating that UNC-119 functions cell-autonomously to suppress axon branching.

Migrating *unc-119* growth cones are morphologically normal

GABA motor neuron axons were branched in *unc-119(ed3)* adults. The simplest explanation for this phenotype is that the axons branched inappropriately during outgrowth. In this case, axon branching would be visible during and shortly after the completion of outgrowth. Alternatively, the branching defects could arise after the axon scaffold had been established. To determine when ectopic axon branching occurred in *unc-119(ed3)* mutants we examined the structure of the DD motor neurons shortly after growth cone migration was completed and again at 48 hours after hatching (Fig. 4). At both of these time points we could distinguish between DD and VD neurons based on cell body location and GFP expression. The DD motor neurons differentiate during embryogenesis and their outgrowth is finished before hatching (Sulston et al., 1983). Surprisingly, we discovered that the majority of DD commissures (58%) were morphologically normal at hatching, that is, they reached the dorsal nerve cord and extended along the dorsal midline. Only 7% of the axons were branched (Fig. 4A,C). However, after 48 hours, branching of the DD axons increased significantly (Fig. 4B,D). Only 25% of axons were normal after 48 hours (n=8 animals, 40 axons scored), while the number of branched axons in mutants had increased to 55%. Thus, DD axon morphology was initially normal but over time DD axons became branched.

These results suggested that GABA motor neuron axon outgrowth was not affected by mutations in the *unc-119* gene. To directly characterize the behavior of elongating motor axons in *unc-119(ed3)* mutants we examined VD-type GABA motor neuron growth cones during outgrowth. The 13 VD motor

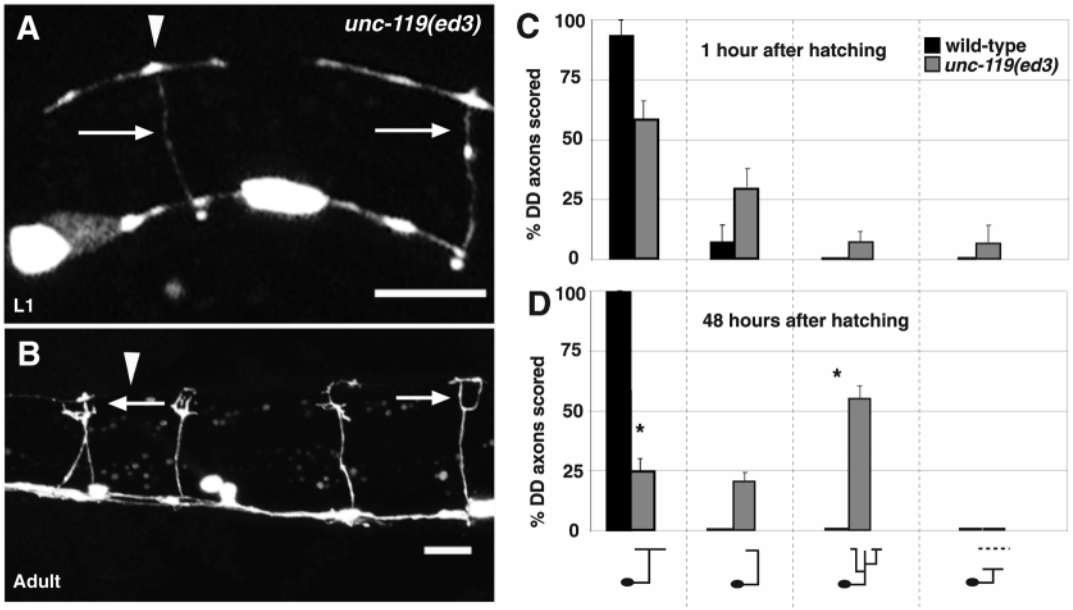

Fig. 4. DD axon morphology changes over time in *unc-119(ed3)* mutants. (A) Confocal micrograph of an *unc-119(ed3)* L1 larvae expressing GFP in the GABA motor neurons. The DD axons (arrows) bifurcated normally at the dorsal nerve cord (arrowhead). (B) The DD neurons in an adult *unc-119(ed3)* mutant were branched (arrows). There were large gaps in the dorsal nerve cord (arrowhead). (C,D). The number of branched DD axons increased over time in *unc-119(ed3)* mutants. (C) At 1 hour after hatching 93% ±3.2 of wild-type axons were normal (left, n=12 worms, 71 axons). Most *unc-119(ed3)* DD axons were also normal at this stage (left, 58% ±8.1, n=15 worms, 79 axons). Some *unc-119(ed3)* axons reached the dorsal nerve cord but failed to extend normally along the dorsal midline (middle left, 28% ±7.2), which was also true for some wild-type axons at this time (7% ±3.2). Only a small fraction of mutant DD axons were visibly branched (middle right, 7% ±4.0), or failed to reach the dorsal nerve cord (right, 7% ±6.7). (D) At 48 hours after hatching, all wild-type axons were morphologically normal (left, n=16 worms, 96 axons). However, the fraction of normal axons in *unc-119(ed3)* mutants was significantly reduced (left, 25% ±8.1, n=8 worms, 40 axons). The fraction of axons that failed to extend along the dorsal midline did not change significantly (middle left, 20% ±3.8). The number of branched axons in *unc-119(ed3)* mutants increased eightfold (middle right, 55% ±5.0). The percentage of axons that failed to reach the dorsal nerve cord did change significantly (0%, right). Significance between time points is indicated by an asterisk (*, P<0.0001, t-test). Error bars represent the standard error of the mean. Scale bars (A,B) 10 μm.

neurons are morphologically and functionally similar to the DD motor neurons, although they differentiate later. The VD motor neurons are born during the first larval stage of development (L1) and extend growth cones to the dorsal cord during the first larval molt (Knobel et al., 1999). We examined the behavior of the VD growth cones by performing time-lapse analysis of migrating growth cones in *unc-119(ed3)* mutants (*n*=13 growth cones). We characterized these growth cones with respect to four specific behaviors: trajectory of migration, growth cone shape changes, the amount of growth cone branching observed during migration and rate of migration. The ventral to dorsal trajectory of VD growth cones was not altered by mutations in *unc-119*. *unc-119(ed3)* VD growth cones also exhibited normal changes in growth cone shape at defined locations along their trajectory (Fig. 5). These behaviors were identical to the shape changes observed during wild-type growth cone migration (Knobel et al., 1999). For example, both wild-type and *unc-119(ed3)* VD growth cones were rounded as they extended across the lateral epidermis. When they contacted a new substrate, these growth cones formed anvil-shaped structures. Both wild-type and *unc-119(ed3)* growth cones extended dorsally directed fingers that projected from the anvil to the dorsal nerve cord. Collapse of the anvil-shaped growth cones occurred when these fingers contacted the dorsal nerve cord. Like wild-type growth cones, some *unc-119(ed3)* growth cones extended multiple fingers toward the dorsal nerve cord (15%). By the time the ventral growth cone had collapsed, only one of these fingers remained in contact with the dorsal nerve cord. At no point did we observe axon branching during *unc-119(ed3)* VD growth cone migration. We did observe that the overall rate of migration of *unc-119(ed3)* VD growth cones is significantly slower than that observed in wild-type worms (*unc-119(ed3)*: 9 μm/hour, range 6-14; wild-type: 26 μm/hour, range 20-55; Knobel et al., 1999). One explanation for this reduction in the rate of growth cone migration is that the rate of *unc-119(ed3)* development is slowed. We observed that *unc-119(ed3)* embryos develop at roughly the same rate as the wild-type although *unc-119(ed3)* mutants hatch later. We believe that the failure to hatch on time is the result of an inability to break through the eggshell due to severe locomotory defects. We observed that the rate of development in *unc-119(ed3)* larvae is reduced: wild-type animals develop into adults 2 days after hatching (~45 hours) at 20°C, whereas *unc-119(ed3)* mutants become adults after 2.5 days (~55 hours). However, the reduction in the rate of postembryonic development does not entirely account for the decrease in growth cone migration rates. Therefore, the reduction in the rate of growth cone migration observed in *unc-119(ed3)* mutants could be attributed to mutations in *unc-119*. In summary, time-lapse analyses revealed that *unc-119(ed3)* growth cones migrate slower than normal but exhibit wild-type morphologies. Most importantly, these studies clearly indicated that axon branching does not occur during growth cone migration in *unc-119(ed3)* mutants.

Supernumerary growth cones are generated from a mature nervous system in *unc-119* mutants

If axon branching in *unc-119(ed3)* mutants does not occur during growth cone migration, then when does it happen? To address this question we characterized the behavior of DD axons between 1 and 48 hours after hatching. Specifically, we determined the nature and timing of any extensions projecting

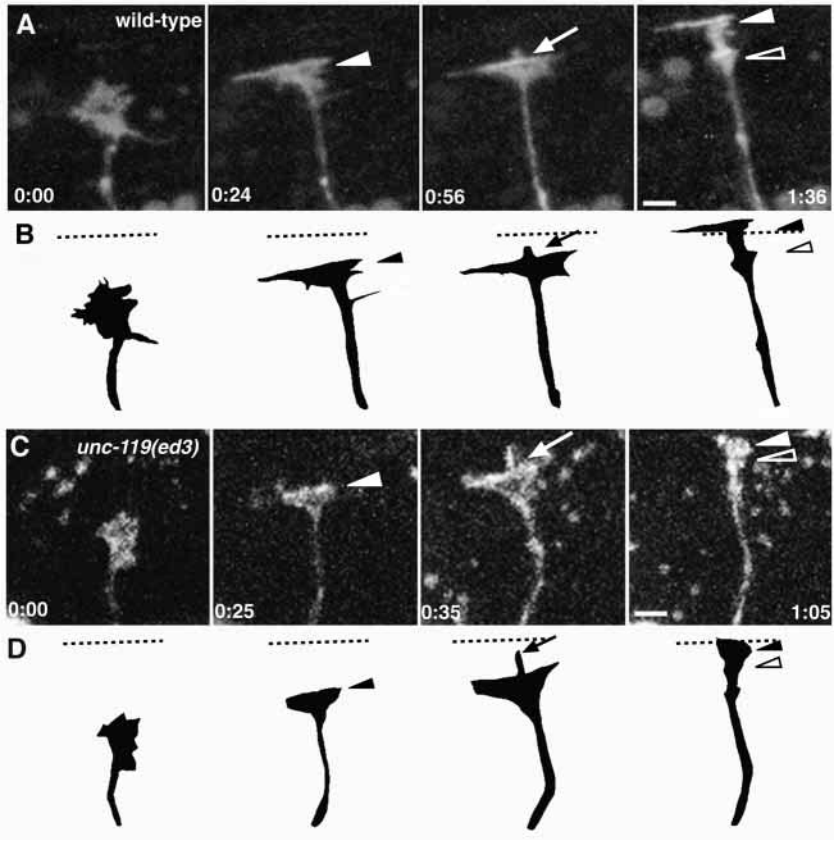

Fig. 5. VD growth cone migration is normal in *unc-119(ed3)* mutants. (A) Time-lapse images of a migrating VD growth cone in a wild-type animal expressing GFP in the GABA motor neurons. At time 0:00, the lateral growth cone was round as it migrated circumferentially across the epidermis. When it contacted the dorsal body wall muscle, the growth cone formed an anvil-shaped structure (arrowhead, 0:24). A single finger extended between the muscle and epidermal cells toward the dorsal nerve cord (solid arrow, 0:56). Eventually this finger contacted the dorsal nerve cord where a new growth cone formed (arrowhead 1:36). The original growth cone located at the ventral side of the body wall muscle was collapsing (open arrowhead). (B) Schematic of wild-type growth cone imaged in A. The dorsal nerve cord is indicated by a dotted line. (C) Time-lapse images of a migrating VD growth cone in an *unc-119(ed3)* mutant expressing GFP in the GABA motor neurons. At 0:00, the lateral growth cone was round. When the growth cone contacted the dorsal body wall muscle (0:25, arrowhead) it formed an anvil-shaped structure. The growth cone sent fingers dorsally (solid arrows, 0:35) that contacted the dorsal nerve cord. At 1:05 the finger reached the dorsal nerve cord where a new growth cone formed. The ventral growth cone (open arrowhead) collapsed. (D) Schematic of *unc-119(ed3)* growth cone imaged in C. The dorsal nerve cord is indicated by a dotted line. Scale bars (A,C) 5 μm.

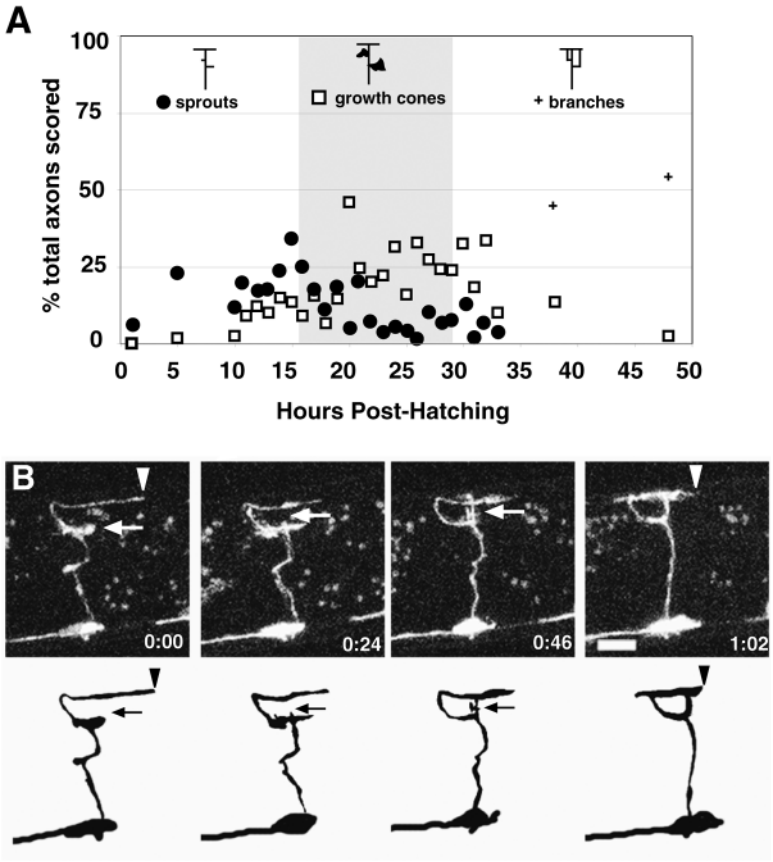

Fig. 6. *unc-119(ed3)* DD axon branches are produced by secondary growth cones. (A) Sprouting from DD axons increased with time. Lateral sprouts (black dots) extending from DD axons were observed before 15 hours in *unc-119(ed3)* mutants expressing GFP in the GABA motor neurons. Sprout activity peaked at 15 hours post-hatching (33%) and was nearly absent by 30 hours after hatching. Growth cones extending from DD axons (open squares) increased in number after 10 hours, by 20 hours 44% of DD axons scored had supernumerary growth cones. Axon branches (+) became visible 30 hours after hatching. VD growth cone migration occurred between 15 and 30 hours after hatching in *unc-119(ed3)* mutants (gray field). During this analysis we did not observe sprouts or axonal growth cones in wild-type animals at any time (*n*=7). (B) Axonal growth cones produced supernumerary branches in *unc-119(ed3)* mutants expressing GFP in the GABA motor neurons. Time-lapse analysis of an *unc-119(ed3)* axon showed an axonal growth cone (arrow, 0:00) extending multiple branches towards the dorsal nerve cord (arrow, 0:24 to 1:02). One of these branches projected to the dorsal nerve cord (arrow, 0:46). Note that the axon extended along the dorsal midline retracted (compare arrowheads in 0:00 and 1:02). Below is a schematic of the growth cone. Scale bar is 5 μm.

from axons (Fig. 6A). We observed three different types of axonal projections in *unc-119(ed3)* mutants: short lateral sprouts, secondary growth cones extending from axons, and axon branches projecting to the dorsal nerve cord. We also observed but did not quantify the extension of supernumerary growth cones from DD cell bodies. Sprouts were observed at almost all time-points in *unc-119(ed3)* mutants. However, the number of sprouts varied at different times; sprouting increased after hatching, peaked at 15 hours (33% of axons possessed sprouts), and then decreased. We also quantified the presence of secondary axonal growth cones over time. The rise and fall of these secondary growth cones followed the production of sprouts by about 10 hours. At 24 hours after hatching we observed that 44% of DD axons possessed secondary growth cones. Finally, axon branches became apparent only after 30 hours post-hatching and increased in number from this point on. We never detected any secondary axonal extensions in wild-type animals scored at the same time points. These analyses suggested that there were three distinct periods of abnormal axon extension and that each was characterized by the presence of a unique type of axonal projection. During the 'early' period (0-15 hours after hatching) lateral sprouts extended from the axon. From 15 to approximately 30 hours after hatching, secondary growth cones projected from the axons and cell bodies of the DD neurons. Interestingly, this is also the period during which VD growth cone migration is occurring in *unc-119(ed3)* mutants. The final stage (30+ hours after hatching) was represented by the appearance of axon branches extending to the dorsal nerve cord. These data suggested that sprouts were transformed into growth cones, and that growth cones produced branches.

We performed time-lapse analysis on DD axons in *unc-119(ed3)* animals to determine if the temporal relationship between sprouts, axonal growth cones and axon branches reflected a physical transformation from one structure to the next. First, we filmed individual DD axons for two hours in the 'early' period (between 5 and 7 hours after hatching). In these experiments, we observed that the majority of *unc-119(ed3)* DD axons did not possess any axonal extensions (66%, *n*=74 axons). The remaining axons possessed short, stable sprouts that did not extend or retract back into the axon. Examination of DD axon behavior between 15 and 30 hours after hatching revealed a reduction in the number of morphologically normal axons (26%, *n*=55 axons). In addition, we observed that sprouts were structurally distinct from axonal growth cones. Specifically, secondary growth cones actively projected lamellipodia and filopodia in all directions as soon as they emerged from the axon. Sprouts only extended and retracted laterally. Moreover, time-lapse analysis of the growth cones confirmed that they eventually form supernumerary branches that extend to the dorsal nerve cord (Fig. 6B). We also observed that during branch formation DD axons retracted their dorsal nerve cord extensions. Finally, we observed that some mature DD neurons extended secondary growth cones from their cell bodies to the dorsal nerve cord. This observation accounts for the presence of extra axons in 15% of adult *unc-119(ed3)* mutants. Together, these timelapse experiments demonstrated three crucial points. First, despite the timing of their appearance, sprouts do not turn into axonal growth cones. Second, axonal growth cones produce extra branches in *unc-119(ed3)* mutants. Third, the presence of supernumerary axons in *unc-119(ed3)* mutants is the direct result of the extension of secondary growth cones from DD cell bodies. These data suggest that the UNC-119 protein functions to suppress axon branching and maintain the structure of the axon scaffold *after* growth cone migration is completed.

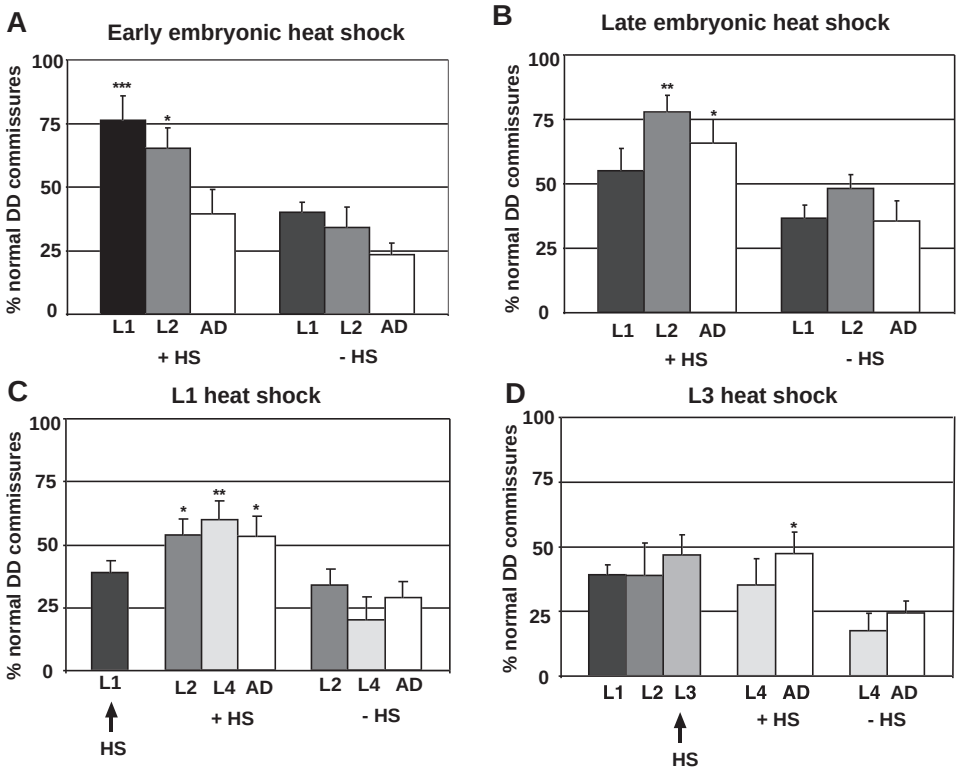

Fig. 7. UNC-119 is required throughout life. (A) Expression of UNC-119 prior to DD axon migration initially rescued the morphology of the DD axons (L1 and L2) relative to non-heat-shocked siblings (–HS). As the animals age, axon morphology declined (AD, adult). *unc-119(ed3)*mutants carrying the [*Phsp*::UNC-119] (+HS) constructs were heat shocked prior to DD axon migration (0-5 hours after fertilization). (B) Expression of UNC-119 after axon migration maintained the morphology of the DD neurons. *unc-119(ed3)* animals carrying the [*Phsp*::UNC-119] constructs were heat shocked after DD axon migration was completed (10-15 hours after fertilization). (C) Expression of UNC-119 during the L1 larval stage restored axon morphology. *unc-119(ed3)* carrying the [*Phsp*::UNC-119] arrays were heat shocked during the L1 larval stage (0-5 hours after hatching). (D) Expression of UNC-119 in the L3 larval stage prevented the decline of axon morphology. *unc-119(ed3)* animals carrying the [*Phsp*::UNC-119] arrays were heat shocked in L3 larval stage (36 hours after hatching). The asterisks indicate significant difference compared to the non-heat-shocked controls as determined by an unpaired *t*-test: *** $P<0.0001$, ** $P< 0.001$, * $P<0.05$.

UNC-119 is required for maintenance of the axon scaffold

In *unc-119 (ed3)* mutants we observed that motor axon branching occurs *after* outgrowth is completed. This observation suggested that the presence of a functional UNC-119 protein is required to suppress axon branching. When is UNC-119 function required? There are three possibilities: (1) UNC-119 could be required during outgrowth only; axons that developed in the absence of UNC-119 may grow out correctly but they are unstable, (2) UNC-119 could be required immediately after outgrowth during differentiation to stabilize the differentiated state, or (3) UNC-119 could be required throughout the life of the animal to maintain neuronal morphology. To distinguish among these possibilities we expressed the UNC-119 protein before, during and after DD outgrowth in *unc-119 (ed3)* mutants using two different heat-shock promoters. We present cumulative data from both heat-shock promoters (see Materials and Methods). When UNC-119 was expressed before DD axons had extended to the dorsal nerve cord (‘early embryonic heat shock’; Fig. 7A) we observed that 24 hours after heat shock the number of morphologically normal axons was increased relative to siblings that did not have heat-shock induced expression of UNC-119. Rescue of axon morphology declined over time so that when these animals molted into adults there was no significant difference between treated and untreated siblings. When embryos were heat shocked after the completion of DD outgrowth (‘late embryonic heat shock’, Fig. 7B), we observed that axon morphology was improved compared to untreated animals. Again, there was a decline in the number of wild-type axons in these animals over time as observed within the early embryonic heat-shock group. Expression of a GFP-tagged UNC-119 protein demonstrated that the fusion protein remained present for approximately 24 hours before fluorescence disappeared, presumably the result of degradation (data not shown). The disappearance of UNC-119::GFP fluorescence coincided with the decline of nervous system morphology. Expression of UNC-119 during the L1 and L3 larval stages demonstrated that expression of UNC-119 even after differentiation was complete could halt the further deterioration of the nervous system (Fig. 7C,D). In short, loss of the UNC-119 protein led to a progressive degeneration of axon morphology during larval stages, and conversely, expression of UNC-119 during larval development was sufficient to maintain nervous system morphology. Surprisingly, the expression of UNC-119 after the morphology of the axons had declined could *reverse* the defects. Specifically, heat shock during the L1 stage resulted in significantly improved morphology (P=0.02 compared to L4; Fig. 7C). These results suggest that even mature neurons whose morphology has declined have the potential to repair defects such as extra branches and thereby reestablish a normal morphology. Interestingly, these DD neurons were reversing their developmental defects during the time when the VD neurons were developing and the DD neurons were rewiring synapses; perhaps this stage represents a period of neuronal plasticity. These data are all consistent with a requirement for UNC-119 throughout the life of the animal.

Table 1. Synapse morphology in the wild type and in *unc-119(ed3)* mutants

Stage/location of synapse	Varicosity width (μm)	Synaptic interval (μm)	Ave no. synapses/ axon scored
DD synapses			
L1/ventral nerve cord			
wild type (*n*=21 worms)	1.4±0.096	2.7±0.15	5.7±0.47
unc-119 (*n*=23)	1.3±0.011	2.3±0.18	3.8±0.44*
L1/dorsal nerve cord			
wild type (*n*=21)	0	0	0
unc-119 (*n*=23)	0.9±0.076*	2.8±0.29*	4.8±1.10*
Young adult/Dorsal nerve cord			
wild type (*n*=10)	1.5±0.05	4.4±0.17	28.9±3.6
unc-119 (*n*=9)	1.5±0.22	4.1±0.89	1.5±1.1*
VD synapses			
Young adult/Ventral nerve cord			
wild type (*n*=8)	1.4±0.062	3.1±0.11	28.5±2.49
unc-119 (*n*=10)	2.2±0.12*	5.3±0.40*	7.5±1.7*

*Significantly different from wild type (unpaired *t*-test, $P<0.0001$).

Synapse formation does not require UNC-119

During neuronal maturation, synapses form at the tip of newly extended axonal processes in vertebrates. To determine if neuromuscular synapses are formed in *unc-119(ed3)* adults we expressed a GFP-tagged synaptic vesicle protein, synaptobrevin (Nonet, 1999) in the GABA motor neurons. In general, the morphologies of *unc-119(ed3)* presynaptic varicosities were similar to those observed in wild-type animals, although there were small but significant differences in varicosity size and distribution in the mutants (Table 1; Fig. 8). The large reduction in the number of varicosities counted along dorsal axons is caused by the loss of motor neuron processes along the dorsal midline in *unc-119(ed3)* mutants. Presumably these were areas where axons failed to extend along the dorsal nerve cord (Fig. 1B) or were retracted after outgrowth (Fig. 6B). Synapses were also observed at lateral locations where branched processes contacted muscles (Fig. 8D). To further establish that functional synapses were formed in *unc-119(ed3)* mutants, we determined whether GABA receptors were clustered in the dorsal and ventral body wall muscles using a GFP-tagged GABA receptor (Bamber et al., 1999). The distribution of postsynaptic receptor clusters closely reflected the pattern of presynaptic varicosities observed in *unc-119(ed3)* (data not shown). These data indicated that pre- and postsynaptic specializations are able to differentiate normally in *unc-119(ed3)* mutants. Finally, we used transmission electron microscopy to analyze synaptic ultrastructure (Fig. 9). Both cholinergic and GABAergic active zones were organized normally in *unc-119* mutants (Fig. 9B, D). Moreover, there is no significant difference in the number of synaptic vesicles associated with the active zone between wild-type and *unc-119(ed3)* mutants (Fig. 9E).

Synapse localization requires UNC-119

Although synapses form in their normal location along the axon in *unc-119* mutants, we discovered that they were also ectopically located in dendritic regions. In newly hatched L1 larvae DD neurons normally receive input from neurons in the dorsal nerve cord and synapse onto muscles in the ventral nerve cord (White et al., 1986). In the wild-type, DD synapses were absent along the dorsal nerve cord (Fig. 10C; Table 1; *n*=20 DD3 axons). However, in *unc-119(ed3)* larvae, 52% of DD axons formed synapses in the dorsal nerve cord (Fig. 10D,E; Table 1; *n*=23 DD3 axons). Neuromuscular junctions were also appropriately located in the ventral nerve cord in newly

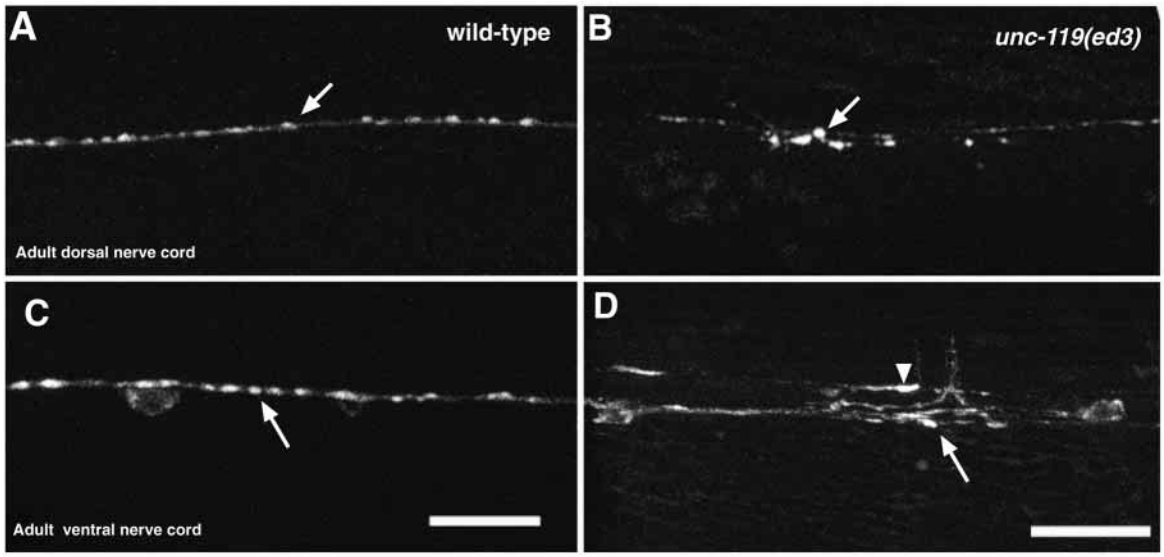

Fig. 8. Synapses are formed in *unc-119(ed3)* mutants. (A) Dorsal view of a wild-type adult animal expressing GFP-tagged synaptobrevin in the DD neurons located in the dorsal nerve cord. DD synapses (arrow) were uniformly distributed along the dorsal nerve cord. (B) Dorsal (DD) synapses in *unc-119(ed3)* young adults were present but discontinuous because of large gaps in the dorsal nerve cord. (C) Ventral view of a wild-type adult expressing GFP-tagged synaptobrevin in the VD synapses of the ventral nerve cord. VD synapses were located along the ventral nerve cord of wild-type worms (arrow). (D) The distribution of VD synapses in the ventral nerve cord of *unc-119* adults was abnormal. A lateral branch that formed synapses is indicated by an arrowhead. Scale bars 10 μm.

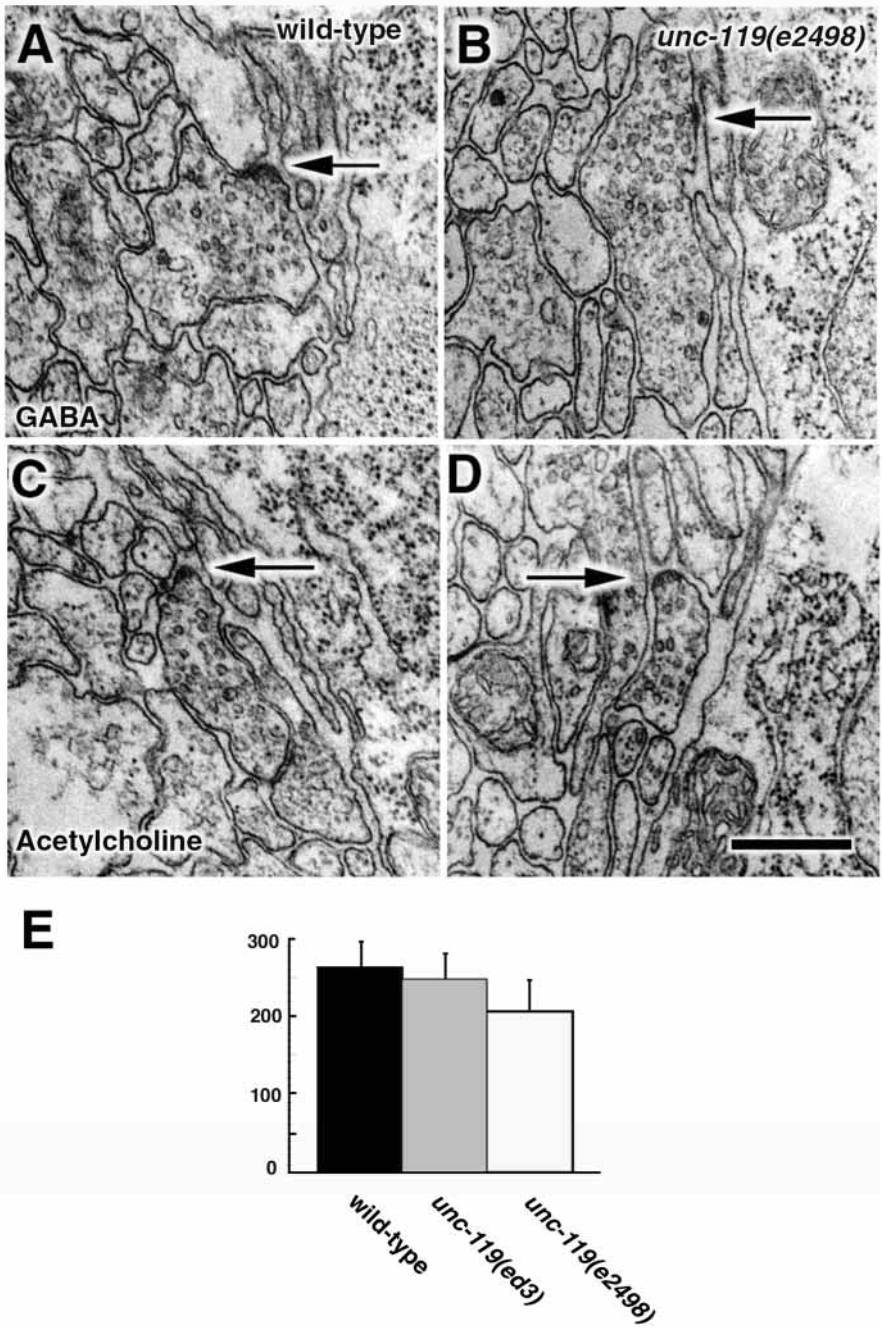

Fig. 9. Synapse ultrastructure is normal in *unc-119* mutants. Presynaptic specializations are indicated. (A) A GABA neuromuscular junction in the ventral nerve cord of a wild-type adult. (B) A GABA neuromuscular junction in the ventral nerve cord of an *unc-119(e2498)* adult. (C) An acetylcholine neuromuscular junction in the ventral nerve cord of a wild-type adult. (D) An acetylcholine neuromuscular junction in the ventral nerve cord of an *unc-119(e2498)* adult. *(E)* The number of synaptic vesicles per active zone was similar in wild type (black, 262±31.8 vesicles per active zone), *unc-119(ed3)*(gray, 246±33.0), and *unc-119(e2498)*(white, 207±39.0). These numbers are not significantly different. Error bars represent standard deviation. Scale bar 10 nm.

hatched *unc-119(ed3)* L1 larvae (Fig. 10B). Dendritic synapses were also found in other neurons in *unc-119* mutants. Synapses were inappropriately located in dendrites of 38% of *unc-119(ed3)* ASI neurons (*n*=8, data not shown), and presynaptic varicosities were found in inappropriate regions of the PLM axon in *unc-119(ed3)* mutants (*n*=5; data not shown). From these experiments we conclude that UNC-119 is required to prevent the localization of synapses in dendrites. Alternatively, these clusters of vesicles might not reflect the position of synapses but might rather be caused by incorrect targeting of synaptic vesicles.

DISCUSSION

The UNC-119 protein is required to suppress hypertrophic branching of axons. Using timelapse video microscopy we determined that there is a reduction in the rate of growth cone migration, but that the morphological behaviors exhibited by migrating growth cones in *unc-119(ed3)* mutants were normal. Surprisingly, hypertrophic branching of axons in *unc-119(ed3)* mutants does not occur during nervous system development but rather *after* development of the nervous system is complete. After the primary growth cone of the developing motorneuron reached its target, secondary growth cones projected from the axon shaft or from the cell body of the neuron to form multiple processes to the dorsal cord. As the axon branched, the original process along the dorsal midline retracted. Retraction of this process led to gaps in the dorsal nerve cord in adult animals. Finally, the UNC-119 protein acts cell intrinsically and is present in the axon shafts of neurons.

Furthermore, UNC-119 protein is continuously required to maintain the structure of the nervous system, even after development of the nervous system is complete. Transient expression of the wild-type protein in mutants during development rescued axon structure in early larval stages, but the morphology of the neurons became abnormal when the UNC-119 protein degraded. Expression during late larval stages prevented the further degeneration of the axon scaffold. Interestingly, expression of the protein in the L1 stage reversed defects of the motor neuron axons, thus demonstrating that these neurons still possessed the potential to develop normally even after their normal period of outgrowth had passed.

How does UNC-119 stabilize the structure of the nervous system? We propose four potential mechanisms for UNC-119 function: activity-dependent stabilization, target-dependent differentiation, regulation of the cytoskeleton or of membrane trafficking, or maintenance of cell polarity.

First, neuronal activity is required for the maintenance of

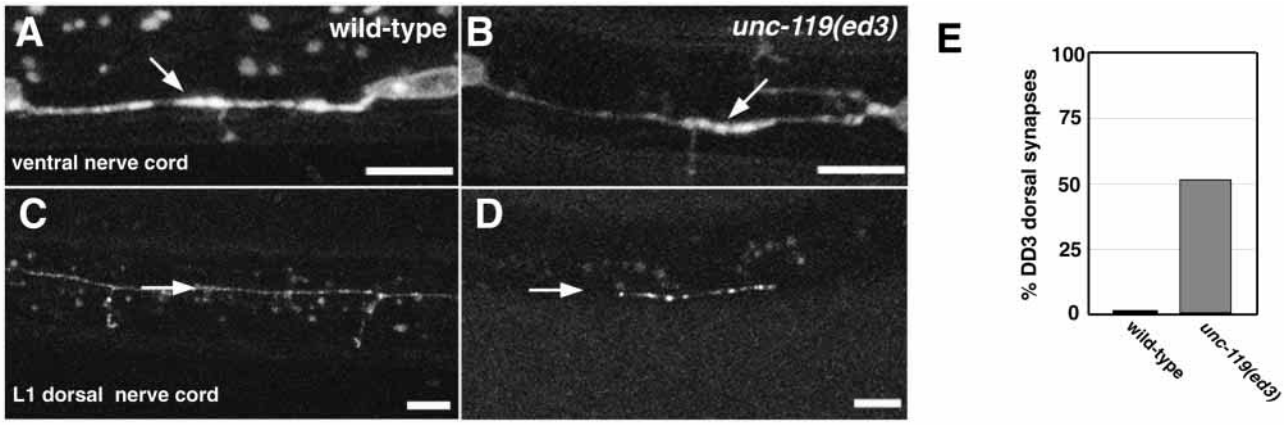

Fig. 10. Synapse localization is disrupted in *unc-119(ed3)* mutants. (A) Ventral view of a newly hatched wild-type L1 larvae expressing GFP-tagged synaptobrevin in DD neurons. Presynaptic varicosities are indicated by an arrow. (B) Ventral view of a newly hatched *unc-119(ed3)* L1 larvae expressing GFP-tagged synaptobrevin in DD neurons (arrow). (C) There were no synaptic varicosities visible in the dorsal nerve cord of wild-type L1 larvae (arrow). (D) Presynaptic varicosities were seen in the dorsal nerve cord of *unc-119(ed3)* mutants (arrow). (E) Dorsal nerve cord varicosities were observed in 52% of *unc-119(ed3)* DD3 axons (wild-type worms: 0% *n*=21 (black); *unc-119*: *n*=23 (gray)). Scale bars (A-D) 5 μm.

nervous system structure in many organisms (Goodman and Shatz, 1993; Katz and Shatz, 1996; Crair, 1999). Increases or decreases in neuronal activity are correlated with excessive axon branching. For example, depolarization of neurons in culture (McCaig, 1990; Perez et al., 1996; Adams et al., 1997; Ramakers et al., 1998) or in living *Drosophila* (Budnik et al., 1990) causes axonal sprouting. Neuronal damage, induced by epileptic seizures or axotomy, results in an increase in synaptic activity and axonal branching of traumatized cells (Lankford et al., 1998; Angelov et al., 1999; McNamara, 1999; Stoll and Muller, 1999). Decreases in neuronal activity can also cause abnormal axon branching. In *C. elegans*, mutations in a cGMP-gated channel or calcium channels cause defects in chemosensory axon morphology (Coburn and Bargmann, 1996; Komatsu et al., 1996; Peckol et al., 1999). Thus, the branching defects observed in *unc-119(ed3)* mutants might be due to a lack of synaptic input into the motor neurons. However, analysis of synaptic function mutants does not support this model. Although weak branching defects in the sensory neurons are observed in the neurotransmission mutant *unc-13* (Peckol et al., 1999), data from our lab indicates that GABA motor neurons are not branched in *unc-13* mutants (Richmond et al., 1999).

Second, the UNC-119 protein might suppress axon branching in response to a differentiation signal. As they approach and contact the target cell, growth cones begin differentiating into functional nerve terminals (reviewed by Burden, 1998; Sanes and Lichtman, 1999). Retrograde signals associated with the synaptic target can initiate the differentiation of the neuron (Dai and Peng, 1996; Fitzsimonds and Poo, 1998; Hall et al., 2000). In *C. elegans*, one source of this differentiation signal may be the body wall muscle. Interestingly, target muscle contact is not required for axon formation (Plunkett et al., 1996). However, muscle contact is necessary for normal synaptogenesis. In fact, the presence of ectopic muscles induces branching of the GABA motor neurons (Plunkett et al., 1996). Thus it is plausible that UNC-119 responds to a target-derived differentiation signal by suppressing further axon outgrowth. In the *unc-119* mutant, failure to receive or transmit this information would cause the neuron to actively branch in search of synaptic targets.

Third, the UNC-119 protein might be required to stabilize the axon, by regulating the cytoskeleton or membrane trafficking in the neuron. For example, it has recently been demonstrated that collateral branch formation involves the local fragmentation of microtubule arrays (Yu et al., 1994; Davenport et al., 1999; Dent et al., 1999). In these regions, fragmented microtubules repolymerize and extend laterally to form interstitial branches. During development, microtubule severing proteins destabilize the cytoskeleton (Quarmby and Lohret, 1999; Quarmby, 2000). One such protein, katanin, is expressed in neurons (Ahmad et al., 1999). It is possible that the UNC-119 protein either inhibits microtubule severing proteins or promotes microtubule stabilizing proteins and thereby preserves axon morphology. Alternatively, UNC-119 might be required for membrane trafficking, perhaps by regulating the targeting of vesicles to the correct compartment of the neuron.

Fourth, UNC-119 may be required to maintain cell polarity. Neurons are highly polarized cells (Craig and Banker, 1994; Higgins et al., 1997). Cell polarity appears to be normal initially in *unc-119* mutants: motor neurons extend a single growth cone that follows the correct trajectory. However, polarity declines thereafter. Secondary growth cones emerge from the shaft and cell body of the neuron. Moreover, distinctions between axonal and dendritic regions break down. Synapses were observed in the dendritic processes of *unc-119* neurons in addition to their normal locations. A differentiated axon tip may exert ‘apical dominance’ on the axon shaft and cell body, analogous to the tip meristem of a plant. Loss of this polarizing signal may lead to the sprouting of multiple axon shafts and the formation of synapses in dendrites.

In summary, many molecules have been identified that are required during axon outgrowth to regulate growth cone behavior and pathfinding. Our studies demonstrate that UNC-119 belongs to a different class of molecules that maintain the differentiated state of the neuron *after* axon outgrowth is completed. Understanding how these molecules function may

eventually reveal the causes of abnormal axon branching in diseased nervous tissue or in response to neuronal trauma.

We are indebted to members of the Salt Lake Area Worm Breeders (SLAWB) group for discussions. In particular, we thank Wayne Davis and Dawn Signor for thoughtful insight and constructive comments on the manuscript. We are grateful to Wayne Materi, Morris Maduro, and David Pilgrim for providing plasmids containing UNC-119 genomic DNA and cDNA as well as information prior to publication. The following people provided reagents and strains for our use: Takeshi Ishihara and Isao Katsura provided the the *acr-5* promoter; Jean-Louis Bessereau constructed *Pacr-5*::GAP-43:GFP (pJL1), *Punc-47*::VAMP:GFP (pJL35), pJL26 (*Phsp16-48*::Matase), and an integrated *oxIs22* strain EG1653; Bruce Bamber made the *Punc-49*::UNC-49B:GFP construct; Yishi Jin provided *juIs1;* Andy Fire provided the original plasmids for all GFP constructs; Gage Crump and Cori Bargmann supplied the *Pstr-3*::synaptobrevin:GFP marker (*kyIs105*); Mike Nonet provided the *Pmec-7*::synaptobrevin:GFP marker (*jsIs37*); Piali Sengupta provided pPD97/98; Marc Hammarlund provided pMH50 (*Paex-3*::SPECTRIN:GFP) and the CGC provided strains for these investigations. We are grateful to Janet Richmond for preparing the worms used in our antibody labeling experiments. Work was initially supported by an NIH Developmental Biology training grant (5T32HD07491) to K. K., and NIH grants NS 34307 to E. M. J. and NS 25387 and NS 02380 to M. J. B.

REFERENCES

Adams, B., Lee, M., Fahnestock, M. and Racine, R. J. (1997). Long-term potentiation trains induce mossy fiber sprouting. *Brain Res.* **775**, 193-197.

Aguayo, A. J., Clarke, D. B., Jelsma, T. N., Kittlerova, P., Friedman, H. C. and Bray, G. M. (1996). Effects of neurotrophins on the survival and regrowth of injured retinal neurons. *Ciba Found. Symp.* **196**, 135-144.

Ahmad, F. J., Yu, W., McNally, F. J. and Baas, P. W. (1999). An essential role for katanin in severing microtubules in the neuron. *J. Cell Biol.* **145**, 305-315.

Angelov, D. N., Skouras, E., Guntinas-Lichius, O., Streppel, M., Popratiloff, A., Walther, M., Klein, J., Stennert, E. and Neiss, W. F. (1999). Contralateral trigeminal nerve lesion reduces polyneuronal muscle innervation after facial nerve repair in rats. *Eur. J. Neurosci.* **11**, 1369-1378.

Bamber, B. A., Beg, A. A., Twyman, R. E. and Jorgensen, E. M. (1999). The *Caenorhabditis elegans unc-49* locus encodes multiple subunits of a heteromultimeric GABA receptor. *J. Neurosci.* **19**, 5348-5359.

Bastmeyer, M. and O'Leary, D. D. (1996). Dynamics of target recognition by interstitial axon branching along developing cortical axons. *J. Neurosci.* **16**, 1450-1459.

Bendotti, C., Vezzani, A., Tarizzo, G. and Samanin, R. (1993). Increased expression of GAP-43, somatostatin, and neuropeptide Y mRNA in the hippocampus during development of hippocampal kindling in rats. *Eur. J. Neurosci.* **5**, 1312-1320.

Bray, D. (1973). Branching patterns of individual sympathetic neurons in culture. *J. Cell Biol.* **56**, 702-712.

Brenner, S. (1974). The genetics of *Caenorhabditis elegans*. *Genetics* **77**, 71-94.

Budnik, V., Zhong, Y. and Wu, C. F. (1990). Morphological plasticity of motor axons in *Drosophila* mutants with altered excitability. *J. Neurosci.* **10**, 3754-3768.

Bunge, M. B. (1973). Fine structure of nerve fibers and growth cones of isolated sympathetic neurons in culture. *J. Cell Biol.* **56**, 713-735.

Burden, S. J. (1998). The formation of neuromuscular synapses. *Genes Dev.* **12**, 133-148.

Caroni, P. (1998). Neuro-regeneration: plasticity for repair and adaptation. *Essays Biochem.* **33**, 53-64.

Chalfie, M., Tu, Y., Euskirchen, G., Ward, W. W. and Prasher, D. C. (1994). Green fluorescent protein as a marker for gene expression. *Science* **263**, 802-805.

Coburn, C. M. and Bargmann, C. I. (1996). A putative cyclic nucleotide-gated channel is required for sensory development and function in *C. elegans*. *Neuron* **17**, 695-706.

Craig, A. M. and Banker, G. (1994). Neuronal polarity. *Annu. Rev. Neurosci.* **17**, 267-310.

Crair, M. C. (1999). Neuronal activity during development: permissive or instructive? *Curr. Opin. Neurobiol.* **9**, 88-93.

Dai, Z. and Peng, H. B. (1996). From neurite to nerve terminal: induction of presynaptic differentiation by target-derived signals. *Semin. Neurosci.* **8**, 97-106.

Davenport, R. W., Thies, E. and Cohen, M. L. (1999). Neuronal growth cone collapse triggers lateral extensions along trailing axons. *Nat. Neurosci.* **2**, 254-259.

Dent, E. W., Callaway, J. L., Szebenyi, G., Baas, P. W. and Kalil, K. (1999). Reorganization and movement of microtubules in axonal growth cones and developing interstitial branches. *J. Neurosci.* **19**, 8894-8908.

Ernfors, P., Bengzon, J., Kokaia, Z., Persson, H. and Lindvall, O. (1991). Increased levels of messenger RNAs for neurotrophic factors in the brain during kindling epileptogenesis. *Neuron* **7**, 165-176.

Fitzsimonds, R. M. and Poo, M. M. (1998). Retrograde signaling in the development and modification of synapses. *Physiol. Rev.* **78**, 143-170.

Goodman, C. S. (1996). Mechanisms and molecules that control growth cone guidance. *Annu. Rev. Neurosci.* **19**, 341-377.

Goodman, C. S. and Shatz, C. J. (1993). Developmental mechanisms that generate precise patterns of neuronal connectivity. *Cell/Neuron* **72/10 (S)**, 77-98.

Goodman, C. S. and Tessier-Lavigne, M. (1997). Molecular mechanisms of axon guidance and target recognition. In *Molecular and Cellular Approaches to Neural Development*, (ed. W. M. Cowan T. M. Jessell and S. L. Zipursky), pp. 108-178. New York: Oxford University Press, Inc.

Hall, A. C., Lucas, F. R. and Salinas, P. C. (2000). Axonal remodeling and synaptic differentiation in the cerebellum is regulated by WNT-7a signaling. *Cell* **100**, 525-535.

Hallam, S. J. and Jin, Y. (1998). *lin-14* regulates the timing of synaptic remodelling in *Caenorhabditis elegans*. *Nature* **395**, 78-82.

Higashide, T. and Inana, G. (1999). Characterization of the gene for HRG4 (UNC119), a novel photoreceptor synaptic protein homologous to Unc-119. *Genomics* **57**, 446-450.

Higashide, T., McLaren, M.J. and Inana, G. (1998). Localization of HRG4, a photoreceptor protein homologous to *Unc-119*, in ribbon synapse. *Invest. Ophthalmol. Vis. Sci.* **39**, 690-698.

Higashide, T., Murakami, A., McLaren, M.J. and Inana, G. (1996). Cloning of the cDNA for a novel photoreceptor protein. *J. Biol. Chem.* **271**, 1797-1804.

Higgins, D., Burack, M., Lein, P. and Banker, G. (1997). Mechanisms of neuronal polarity. *Curr. Opin. Neurobiol.* **7**, 599-604.

Katz, L. C. and Shatz, C. J. (1996). Synaptic activity and the construction of cortical circuits. *Science* **274**, 1133-1138.

Knobel, K. M., Jorgensen, E. M. and Bastiani, M. J. (1999). Growth cones stall and collapse during axon outgrowth in *Caenorhabditis elegans*. *Development* **126**, 4489-4498.

Komatsu, H., Mori, I., Rhee, J.-S., Akaike, N. and Ohshima, Y. (1996). Mutations in a cyclic nucleotide-gated channel lead to abnormal thermosensation and chemosensation in *C. elegans*. *Neuron* **17**, 707-718.

Lankford, K. L., Waxman, S. G. and Kocsis, J. D. (1998). Mechanisms of enhancement of neurite regeneration in vitro following a conditioning sciatic nerve lesion. *J. Comp. Neurol.* **391**, 11-29.

Lewis, J. A. and Fleming, J. T. (1995). Basic culture techniques. In *Caenorhabditis elegans: Modern Biological Analysis of an Organism*, vol. 48 (ed. H. F. Epstein and D. C. Shakes), pp. 3-27. San Diego: Academic Press, Inc.

Maduro, M. A. and Pilgrim, D. (1995). Identification and cloning of *unc-119*, a gene expressed in the *Caenorhabditis elegans* nervous system. *Genetics* **141**, 977-988.

Maduro, M. F., Gordon, M., Jacobs, R. and Pilgrim, D. B. (2000). The UNC-119 family of neural proteins is functionally conserved between humans, Drosophila and C. elegans. *J. Neurogenet.* **13**, 191-212.

McCaig, C. D. (1990). Nerve branching is induced and oriented by a small applied electric field. *J. Cell Sci.* **95**, 605-615.

McIntire, S. L., Reimer, R. J., Schuske, K., Edwards, R. H. and Jorgensen, E. M. (1997). Identification and characterization of the vesicular GABA transporter. *Nature* **389**, 870-876.

McNamara, J. O. (1999). Emerging insights into the genesis of epilepsy. *Nature* **399**, A15-22.

Mello, C. and Fire, A. (1995). DNA transformation. *Methods Cell Biol.* **48**, 451-482.

Mello, C. C., Kramer, J. M., Stinchcomb, D. and Ambros, V. (1991).

Efficient gene transfer in *C. elegans*: extrachromosomal maintenance and the integration of transforming sequences. *EMBO J.* **10**, 3959-3970.

Miyabayashi, T., Palfreyman, M. T., Sluder, A. E., Slack, F. and Sengupta, P. (1999). Expression and function of members of a divergent nuclear receptor family in Caenorhabditis elegans. *Dev. Biol.* **215**, 314-331.

Mueller, B. K. (1999). Growth cone guidance: first steps towards a deeper understanding. *Annu. Rev. Neurosci.* **22**, 351-388.

Nonet, M. L. (1999). Visualization of synaptic specializations in live *C. elegans* with synaptic vesicle protein-GFP fusions. *J. Neurosci. Methods* **89**, 33-40.

O'Leary, D. D. (1992). Development of connectional diversity and specificity in the mammalian brain by the pruning of collateral projections. *Curr. Opin. Neurobiol.* **2**, 70-77.

O'Leary, D. D. and Terashima, T. (1988). Cortical axons branch to multiple subcortical targets by interstitial axon budding: implications for target recognition and "waiting periods". *Neuron* **1**, 901-910.

Peckol, E. L., Zallen, J. A., Yarrow, J. C. and Bargmann, C. I. (1999). Sensory activity affects sensory axon development in *C. elegans*. *Development* **126**, 1891-1902.

Perez, Y., Morin, F., Beaulieu, C. and Lacaille, J. C. (1996). Axonal sprouting of CA1 pyramidal cells in hyperexcitable hippocampal slices of kainate-treated rats. *Eur. J. Neurosci.* **8**, 736-748.

Plunkett, J. A., Simmons, R. B. and Walthall, W. W. (1996). Dynamic interactions between nerve and muscle in Caenorhabditis elegans. *Dev. Biol.* **175**, 154-165.

Quarmby, L. (2000). Cellular Samurai: katanin and the severing of microtubules. *J. Cell Sci.* **113**, 2821-2827.

Quarmby, L. M. and Lohret, T. A. (1999). Microtubule severing. *Cell Motil. Cytoskel.* **43**, 1-9.

Ramakers, G. J. A., Winter, J., Hoogland, T. M., Lequin, M. B., van Hulten, P., van Pelt, J. and Pool, C. W. (1998). Depolarization stimulates lamellipodia formation and axonal but not dendritic branching in cultured rate cerebral cortex neurons. *Dev. Brain Res.* **108**, 205-216.

Richmond, J. E., Davis, W. S. and Jorgensen, E. M. (1999). UNC-13 is required for synaptic vesicle fusion in C. elegans. *Nat. Neurosci.* **2**, 959-964.

Richmond, J. E. and Jorgensen, E. M. (1999). One GABA and two acetylcholine receptors function at the *C. elegans* neuromuscular junction. *Nat. Neurosci.* **2**, 791-797.

Sanes, J. R. and Lichtman, J. W. (1999). Development of the vertebrate neuromuscular junction. *Annu. Rev. Neurosci.* **22**, 389-442.

Sanes, J. R. and Scheller, R. H. (1997). Synapse formation: a molecular perspective. In *Molecular and cellular approaches to neural development*, (ed. W. M. Cowan T. M. Jessell and S. L. Zipursky), pp. 179-219. New York: Oxford University Press, Inc.

Stoll, G. and Muller, H. W. (1999). Nerve injury, axonal degeneration and neural regeneration: basic insights. *Brain Pathol.* **9**, 313-325.

Stringham, E. G., Dixon, D. K., Jones, D. and Candido, E. P. M. (1992). Temporal and spatial expression patterns of the small heat shock (hsp16) genes in transgenic *Caenorhabditis elegans*. *Mol. Biol. Cell* **3**, 221-233.

Sulston, J. E., Schierenberg, E., White, J. G. and Thomson, J. N. (1983). The embryonic lineage of the nematode *Caenorhabditis elegans*. *Dev. Biol.* **100**, 64-119.

Swanson, D. A., Chang, J. T., Campochiaro, P. A., Zack, D. J. and Valle, D. (1998). Mammalian orthologs of *C. elegans unc-119* are highly expressed in photoreceptors. *Invest. Ophthalmol. Vis. Sci.* **39**, 2085-2094.

White, J. G., Southgate, E., Thomson, J. N. and Brenner, S. (1986). The structure of the nervous system of *Caenorhabditis elegans*. *Phil. Trans. Royal Soc. (Lond.)* **B**, 1-340.

Winnier, A. R., Meir, J. Y.-J., Ross, J. M., Tavernarakis, N., Driscoll, M., Ishihara, T., Katsura, I. and Miller, D. M. I. (1999). UNC-4/UNC-37-dependent repression of motor neuron-specific genes controls synaptic choice in *Caenorhabditis elegans*. *Genes Dev.* **13**, 2774-2786.

Yu, W., Ahmad, F. J. and Baas, P. W. (1994). Microtubule fragmentation and partitioning in the axon during collateral branch formation. *J. Neurosci.* **14**, 5872-5884.